

# Evaluation of Energy Conversion and Distribution on the SI-PFI Engine Fueled by A Gasoline-Bioethanol Blend with AFR Variations

Marthen PALOBORAN\*, Thesya Atarezcha PANGRURUK\*\*, Yunus TJANDI\*\*\*

\*Automotive Engineering Education Department, Universitas Negeri Makassar, Makassar, Indonesia,

E-mail: marthen.paloboran@unm.ac.id (Corresponding author)

\*\*Statistics Department, Mulawarman University, Samarinda, Indonesia

\*\*\*Electrical Engineering Education Department, Universitas Negeri Makassar, Makassar, Indonesia

<https://doi.org/10.5755/j02.mech.37170>

## 1. Introduction

Sustainability initiatives aimed at decreasing hydrocarbon emissions from the combustion of fossil fuels will persist in various areas, such as the design of engines, the implementation of advanced technology for combustion control, and the adjustment of combustion parameters. The effectiveness of complete combustion is heavily influenced by the availability of sufficient combustion air to ignite all parts of the fuel injected into the combustion chamber [1-2]. The necessity for combustion air is contingent upon the makeup and quantity of the components that comprise the fuel, whether hydrocarbon or bio-hydrocarbon, as indicated by the fuel compound formula [3]. The amount of required combustion air is generally expressed in terms of the ratio of air to fuel, expressed in units of air mass per mass of fuel (kg/kg). It is considered sufficient when it enables the complete combustion or oxidation of all the injected fuel without leaving behind excess oxygen or unburned fuel, which is typically referred to as stoichiometric AFR [1, 3].

A stoichiometric air-fuel ratio (AFR) is essential for complete combustion, but in practical application, both rich and lean mixtures are necessary for certain conditions. Lifeng Zhao [4] conducted combustion tests on a gasoline and 20% ethanol mixture in a gasoline direct injection engine (GDI) under stoichiometric and lean combustion conditions. The results showed that combustion efficiency increased with lean combustion at an excess air coefficient of 1.2–1.3. Furthermore, the E20 fuel consumption rate was 5% lower than that of gasoline combustion under the same excess air conditions. Meanwhile, research conducted by Odunlami et al. [5] explains that most motorbikes in Nigeria operate at lambda values greater than 1 or rich mixture conditions, where the actual AFR > ideal AFR. This triggers an increase in atmospheric HC, CO, and CO<sub>2</sub> emissions. Meanwhile, an increase in NO<sub>x</sub> emissions is triggered when the mixture is poor or the actual AFR < ideal AFR; thus, there is no ideal AFR value to reduce all emissions produced by diesel and gasoline engines [6].

The relationship between emissions from burning gasoline and lambda and AFR values was studied in depth by Al-Arkawaz [7]. The research was conducted on motorized vehicles in Iraq for six types of fuel volume capacities. The results show that O<sub>2</sub> emissions will decrease if the lambda value increases, and if all the O<sub>2</sub> is absorbed by the fuel, complete combustion will occur, and combustion produces only water vapor and CO<sub>2</sub>. The CO<sub>2</sub> and CO emissions decrease if the lambda value increases, while NO<sub>x</sub> emissions are not affected by increasing the lambda value

[8]. Fuel combustion emissions in internal combustion engines can be predicted by carefully calculating the AFR of the fuel [9]. The accuracy of the calculation is at least influenced by several factors, namely, NO<sub>x</sub> emissions, whose value does not significantly affect the AFR value; the assumed value of the water and gas equilibrium constant (K), where variations in the K value from 2-6 will affect the calculation of the AFR value by 2%; air temperature and relative humidity by 1%; and equipment errors.

The air-fuel ratio plays a critical role in determining the quality of combustion and fuel consumption of an engine, as demonstrated by Frasci et al. [10]. When a turbulent jet ignition (TJI) system is implemented in a spark ignition engine, an increase in the Lambda value from 1.0 to 1.6 leads to slower combustion. However, the maximum increase in the HRR value can be reduced. Furthermore, the application of TJI results in faster combustion compared to conventional systems under suboptimal combustion conditions [11], thereby improving the combustion quality. Few research results specifically examine the air-fuel ratio to produce stoichiometric combustion other than those mentioned above. Therefore, this research was conducted in addition to validating the AFR value for a mixture of gasoline and bioethanol fuel in a balanced composition to produce high engine performance and low emissions. This study was also very useful as a prime reference material in the combustion field with varying air-fuel ratios.

## 2. Literature Review

### 2.1. Bioethanol and internal combustion engine

Bioethanol as a substitute for gasoline fuel to spark ignition engines is widely used in several countries, especially in Latin America [12]. Bioethanol is also widely used as a mixed fuel with gasoline, diesel, and other fuels in various blends. Research by Bhaskar Paluri et al. [13] revealed that the heat of combustion, fuel consumption, and peak combustion pressure increased with increasing bioethanol concentration in gasoline. This research is linear with the research of Rimkus et al. [14] and Paloboran et al. [15-16], who conducted an in-depth study on the use of E0, E50, E70, E85, and E100 fuels. Furthermore, Suyatno et al. [17] have conducted a study on the use of isooctane fuel and a mixture of bioethanol and isooctane 50:50% at various ignition timings of 9, 12, and 15 bTDC. The results show that engine performance increases at an ignition timing of 12 bTDC for a mixture of isooctane and bioethanol fuel. Furthermore, the best engine performance is obtained when

using isoctane fuel at an ignition timing of 9 bTDC, except that energy consumption, CO, and HC emissions are worse than the others. A decade before Suyatno, the use of isoctane fuel was also carried out by J. Serras-Pereira et al. [18] in a spark ignition-direct injection engine. The results show that the isoctane combustion process is slower than ethanol fuel.

Two countries in South America namely USA and Brazil were the largest producers and used bioethanol for vehicles and have long been developing FFV fueled by E27 as mandatory, E85, and even E100. A study was conducted by Felipe S. Frutuoso et. al. [19], who examined the performance of FFV BRT in the city of Fortaleza. The results show that CO<sub>2</sub> is the largest emission produced by vehicles for all types of fuel. The highest NO<sub>x</sub> emissions are produced by E100 fuel, while the highest CO emissions are produced by E85. One way to improve the performance of an ethanol-fueled SI engine at varying lambda is to use supercharge. This was proven by Constantin Pana et al. [20] in their research using a 1.5L capacity SI engine fueled by E20. The results show that the power and pressure of the E20-fueled engine are higher than that of gasoline fuel at the same lambda value. Likewise, CO, HC, NO<sub>x</sub>, and ISFC emissions from E20 fuel are lower than E0, although NO<sub>x</sub> emissions in E20 tend to increase if the lambda value is < 1 [21].

Fuel quality also greatly influences fuel consumption, AFR, Lambda, and gasoline engine emissions. It was stated by Flamarz Al-Arkawazi [22], who researched gasoline-fueled GDI engines. The research results show that a high fuel octane value will cause increased fuel consumption. Furthermore, the AFR value will decrease if the benzene and aromatics content in gasoline increases, and this will also cause an increase in CO<sub>2</sub> emissions. The increase of benzene and aromatic compounds in gasoline causes the AFR and lambda values to reach stoichiometric conditions, resulting in complete combustion. The use of various types of alternative fuels in gasoline engines as an effort to reduce hydrocarbon emissions will have an impact on the friction and wear of internal combustion engines [23]. In addition, in the long term, it will cause corrosion and chemical as well as tribochemical changes in the fuel mixture [24].

## 2.2. Energy balance and operational defenition of research variable

The combustion process in an internal combustion engine always strives for the energy contained in the fuel to be maximally converted to useful energy, which is measured through indicative power and shaft power parameters. Apart from being converted into indicative power, the energy produced from the thermochemical process of fuel will also be lost and wasted into the environment through the heat transfer process, cooling system, and wasted energy through exhaust gas. Furthermore, the indicative power produced through the combustion process is converted into work to move the engine, and some of it is lost through friction, pumping, transmission system losses, etc. The energy balance in an internal combustion engine is shown via a Sankey diagram as shown in Fig. 1.

### 2.2.1. Fuel energy

In an internal combustion engine, air and fuel will blend and form a mixture that will ignite through a spark for a spark ignition engine or gasoline engine and through cylinder pressure for a diesel engine. As the mixture of air and fuel burns, a certain amount of heat will be produced. Furthermore, the amount of heat is influenced by several factors, one of which is the composition of the compounds contained in the fuel. Moreover, the fuel energy is also influenced by the type of carbon and hydrogen bonds in the compound. For example, in hydrocarbon fuels, the energy produced by methane (CH<sub>4</sub>) is different from decane, C<sub>10</sub>H<sub>22</sub> [25].

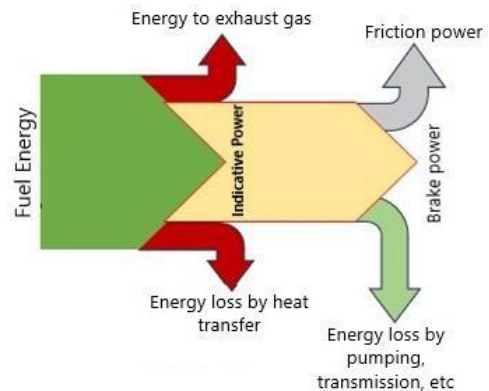


Fig. 1 Sankey diagram of energy balance in ICE

The quantity of energy released by fuel during the combustion process is determined by the Low Heating Value (LHV) or net calorific value of the fuel, and it is expressed in units of megajoules per kilogram (MJ/kg). The relationship between the LHV values of various types of fuel and the stoichiometric AFR values is shown in Fig. 2. The figure shows that the LHV values for several types of hydrocarbon fuel do not differ significantly. In contrast, fuels whose substance consists of oxygen compounds have a lower LHV value than hydrocarbon fuels, so the AFR value is lower than hydrocarbon fuels [26].

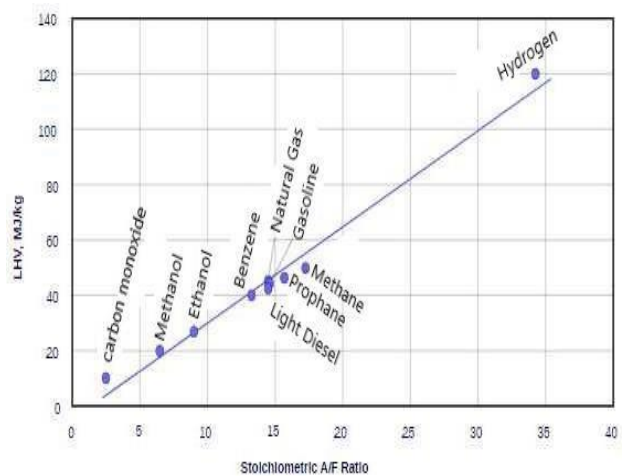


Fig. 2 LHV of various fuel types versus AFR values [25]

### 2.2.2. Indicative power

Indicative power is the power produced by the engine in the process of burning fuel in the cylinder in the form

of heat. In the combustion process, not all of the fuel energy can be converted into indicative power, but some of the energy will be lost through heat transfer and cooling processes and will exit through exhaust gases.

### 2.2.3. Brake power

Brake power is the energy that is converted into useful power to drive the engine and expressed in kilowatts (kW). Based on Fig. 1, brake power is the difference between indicative power and friction losses, pumping losses, and losses in transmission systems.

### 2.2.4. Energy losses

Energy loss is energy that cannot be utilized as useful power. Energy loss is caused by several factors, namely technical factors that consist of materials, machine construction, cooling systems, insulation systems, heat distribution, and utilization systems, as well as operational factors, including combustion systems.

## 3. Materials and Experiment Setup

The engine is operated at constant load and speed, namely 3 Nm and 1500 RPM, respectively. This condition was deliberately chosen to see other engine parameters when the engine is at peak power (1800 RPM). The fuel used is a mixture of gasoline (in Indonesia called Pertalite,  $C_8H_{12}$ ) and bioethanol ( $C_2H_5OH$ ) with a composition of 50%: 50% on a mass basis. The calorific value of the blend (E50) is 34.8 MJ/kg [27], which is properties as shown in Table 1. Meanwhile, the compression ratio used is 10:1 with standard ignition and AFR variations of 10:1, 12:1, and 14:1. Specification of the test engine is shown in Table 2, while the error uncertainties for all measuring instruments used are shown in Table 3.

Table 1

Test fuel properties [14]

Fuel/Properties	Gasoline	Bioethanol
Chemical formula	$C_8H_{12}$	$C_2H_5OH$
Elements composition, %:		
Carbon ©	86.00	52.14
Hydrogen (H)	13.998	13.13
Oxygen (O)	0.002	34.73
C/H	6.15	3.97
Density (20°C), kg/m <sup>3</sup>	736	790
Viscosity (40°C), mm <sup>2</sup> /s	0.4–0.8	1.13
Latent heat of evaporation, kJ/kg	364	840
Laminar flame speed, cm/s	51	63
AFR	14.84	9.10
Auto-ignition temperature, °C	257	422
Lower heating value, MJ/kg	43.5	27.0
Octane Number	88-98	109
Boiling point, °C	27-225	78

## 4. Results and Discussion

### 4.1. Fuel energy rate

Fuel is a substance or material that can be burned and produces energy in the form of heat or power [28]. The amount of energy produced depends on the elements and compounds that make up the fuel, which are also used as indicators of fuel quality with certain standards. Figs. 4 and

5 show the fuel energy produced from the E0 and E50 combustion processes at engine speeds of 1500 and 1800 RPM with a constant load of 3 kg. Even though the LHV of E50 fuel is lower than E0, the quantity of heat produced by E50 is higher than E0 if the air-fuel ratio is 14:1, both at 1500 RPM and 1800 RPM. This condition proves that theoretically, the stoichiometric air-fuel ratio of E50 is between E0 (14:1) and E100 (9:1), which is around 12.5:1, but in reality, the E50 fuel energy is obtained at AFR 14:1, both at high or low engine speeds. The absolute error and uncertainty values of each measuring instrument used are included in this study; which state the difference between the measurement results and the actual value [42], as shown in Table 3.

Meanwhile, the E50 fuel energy at AFR 10:1 tends to be the same as AFR 12:1 and smaller than E0, as shown in Fig. 4. Fig. 5 shows that the E50 fuel energy increases

Table 2

The specification of the engine and apparatus

Type of engine	4 strokes, SOHC
Number of cylinders	1
Length of stroke	110 mm
Bore diameter	87.5 mm
Cylinder volume	661 cm <sup>3</sup>
Length of connecting rod	234 mm
Maximum power	3.5 kW/1500 RPM
Speed range	1200 – 1800
Compression ratio range	6:1 – 10:1
Injection variation	0 – 25° bTDC
Dynamometer type	Eddy current
Software	ICEngineSoft
Piezo sensor	Range: 5000 Psi

Table 3

Uncertainty and absolute error of measured parameters

Measured parameter	Uncertainty (%)	Absolute error
Engine speed	1	15 rev/min
Load (kg)	0.25	-
Pressure (bar)	0.5	-
Air flow rate	2.05	99.16 cm <sup>3</sup> /s
Fuel flow rate	2.06	1.28 x 10 <sup>-2</sup> m <sup>3</sup> /h
Engine torque	2	0.6 N m
Temperature	1.57	0.55°C



Fig. 3 Engine test rig

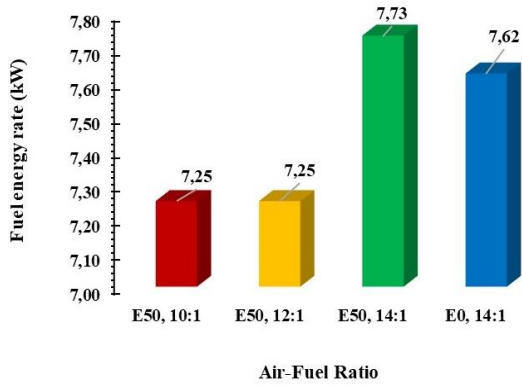


Fig. 4 Fuel energy rate with AFR variations at 1500 RPM

from 1500 RPM to 1800 RPM, and it is higher than E0, especially at AFR 12:1 and 14:1. Meanwhile, at AFR 10:1, the energy of E50 fuel is still smaller than E0 fuel. It illustrates that E50 fuel requires a higher temperature to produce high energy because the latent heat of vaporization of E50 is higher than E0, namely 924 kJ/kg: 400 kJ/kg [29]. It is confirmed by Figs. 4 and 5, where increasing engine RPM has a significant impact on increasing fuel energy by an average of 17% - 23% for both E0 and E50 fuels.

4.2. Indicative power

Indicative power is the power in the engine cylinder resulting from the fuel combustion process, or in other words, indicative power is the amount of fuel energy converted into heat in the cylinder. Therefore, not all of the fuel energy can be converted into indicative power, but some will be released into the environment through various heat transfer modes [30]. Figs. 6 and 7 show the fuel energy E0 and E50 converted into indicative power and energy lost through the cooling system, exhaust gas, and heat transfer with the environment at varying AFR. The fuel energy converted into IP (indicative power) decreases with increasing combustion AFR for E50, whose value is higher than E0 for all AFRs, both at 1500 RPM and 1800 RPM [31] as seen in Figs. 6 and 7.

4.3. Energy losses

The average loss of fuel energy wasted in the engine cooling process is 20%, which tends to decrease with increasing engine speed and AFR [32]. It indicates that the

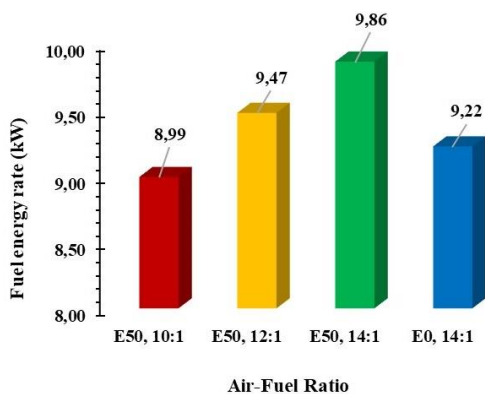


Fig. 5 Fuel energy rate with AFR variations at 1800 RPM

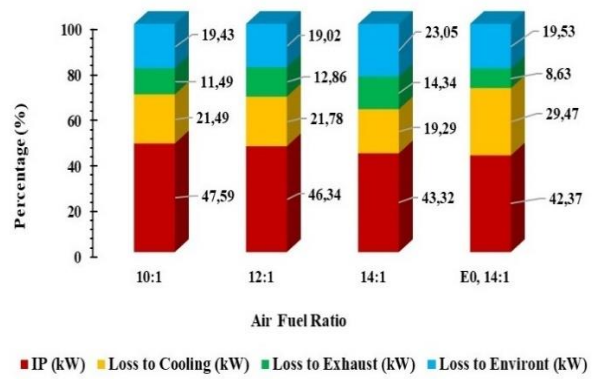


Fig. 6 Conversion of fuel energy at 1500 RPM

heat difference between the system or combustion chamber and the cooling system decreases with increasing the AFR, so the heat flow to the cooling system also decreases [33]. The evaporation pressure of bioethanol is higher than gasoline, so it is one of the causes of energy losses of E50 in the cooling system is lower than E0 [34]. Figs. 6 and 7 also show that the heat energy absorption in the cooling system decreases with increasing engine speed for both E0 and E50 fuels. However, this condition has the consequence of increasing heat loss on the cylinder walls through the conduction heat transfer process. The results also found that heat loss through the cylinder walls increased with increasing engine speed and AFR for E50 and E0 fuels caused the friction to increase [35].

The high energy wasted through the stack indicates that the heat produced from the fuel combustion process cannot be converted into useful power in an energy generation system [36]. Therefore, to reduce heat loss in

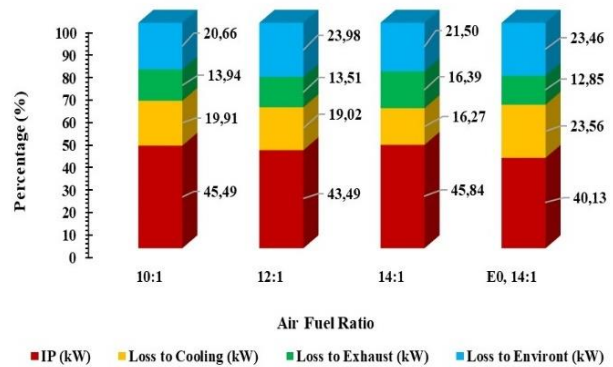


Fig. 7 Conversion of fuel energy at 1800 RPM

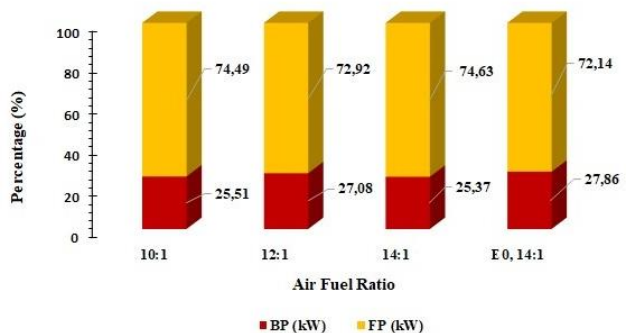


Fig. 8 Conversion of IP to BP and FP at 1500 RPM

exhaust gases, the system can utilize the energy through a heat recovery process so that the system's thermal efficiency can increase [37]. Figs. 6 and 7 also show that heat loss in the exhaust gas increases with increasing AFR and engine speed. This is because the air and fuel mixture also increase with increasing AFR. Furthermore, the cylinder temperature will increase with increasing engine speed so that the energy produced in the form of heat also increases. Heat loss in exhaust gas for E0 fuel is higher than for E50 because the calorific value of E0 fuel is higher than E50.

#### 4.4. Brake and Friction Power

Brake power is indicative power in the form of heat energy in the cylinder that is converted into actual power on the output shaft to move the vehicle or engine load, as seen in Fig. 1. Based on this, the indicative power delivered into brake power is around 25% on average, both at low and high engine speeds, while around 75% becomes friction loss, as seen in Figs. 8 and 9. Indicative power converted into brake power tends to increase at an AFR of 12:1 and AFR of 14:1 for the E50, while at an AFR of 10:1, it tends to decrease for E50 and E0 fuels. The low indicative power converted into shaft power is due to the high frictional power in the system [38]. It can be caused by the viscosity of the lubricating oil being too high, causing friction between the piston and the cylinder wall through the lubricating oil to increase. Therefore, reducing friction losses in internal combustion engines can be done by decreasing the viscosity of the lubricating oil or adding certain additives to the lubricating oil [39].

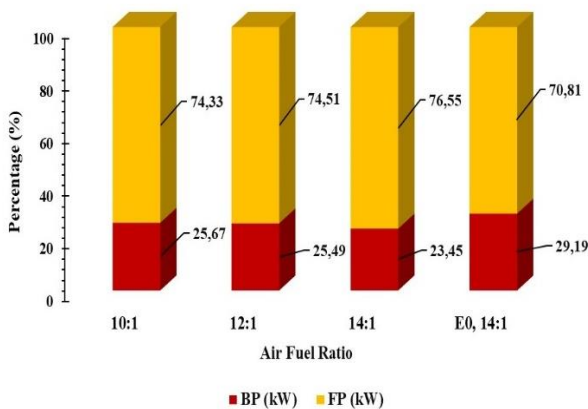


Fig. 9 Conversion of IP to BP and FP at 1800 RPM

#### 4.5. Efficiencies

Efficiency is one indicator of energy performance in optimizing the utilization of all the components in the system. One of the aims of the thermal generation process is carried out through a combustion process to produce high thermal efficiency. The performance of internal combustion engines (ICE) that are used to drive vehicles is measured in at least four efficiency parameters, i.e. indicative thermal efficiency, brake thermal efficiency, mechanical efficiency, and volumetric efficiency. Figs. 10 and 11 show various efficiency indicators for burning E0 and E50 fuel under varying air-fuel ratios. The indicative thermal efficiency of E50 fuel decreases with increasing AFR from 10:1 to 12:1 at 1500 RPM but will reach its peak at AFR 14:1 and an engine speed of 1800 RPM. Meanwhile, the indicative thermal ef-

iciency of E0 fuel decreases as engine speed increases. Indicative thermal efficiency is an indicator of the potential energy of fuel that can be optimized to become heat in the cylinder [40]. The indicative thermal efficiency value depends on the amount of heat loss in the flue gas and energy loss due to heat transfer, as shown in Figs. 6 and 7.

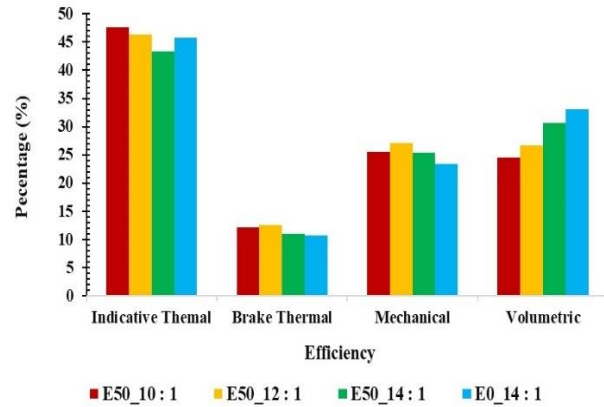


Fig. 10 Various types of efficiency at 1500 RPM

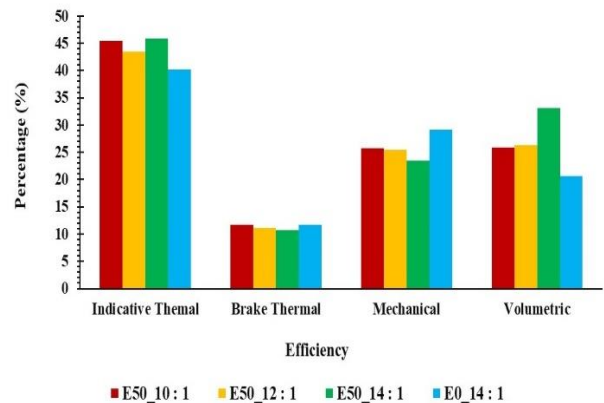


Fig. 11 Various types of efficiency at 1800 RPM

Meanwhile, brake thermal efficiency is the ratio of the power on the output shaft and the energy generated in the combustion process. In research, brake thermal efficiency appears to decrease with increasing AFR at both low and high RPM. This is caused by increased friction in the cylinder due to the high viscosity of the lubricating oil and increased temperature in the cylinder. Figs. 10 and 11 also show the mechanical efficiency of the system that tends to decrease with increasing AFR and engine speed. The decrease in mechanical efficiency is also influenced by the increase in friction losses during the process [41]. Moreover, volumetric efficiency indicates the volume of the air mixture that fills the combustion chamber volume, the value of which increases with increasing AFR and engine speed on E50 fuel, whereas for E0 fuel, it will decrease with increasing engine speed.

## 5. Conclusions

Theoretically, the stoichiometric air-fuel ratio of E50 is 12.5:1. However, it has been found that the optimal combustion performance of E50 in a 662 cc, single cylinder, and spark ignition engine was at AFR 14:1. Some important indicators from the results of this research are as follows:

1. The fuel energy of E50 increases by 1.5% at 1500 RPM and 6.9% at 1800 RPM compared to gasoline fuel at AFR 14:1. Even though the calorific value of E50 is 21% smaller than E0 fuel, the latent heat of vaporization of bioethanol, which is 60% higher than gasoline, makes the high contribution to increasing fuel energy if applied to AFR 14:1.
2. The amount of E50 fuel energy converted into heat energy in the cylinder at AFR 14:1 will be lower than at AFR 12:1 and 10:1. However, the indicative power of E50 is still higher than that of E0 fuel at 1500 RPM and 1800 RPM.
3. Heat loss in the E50 fuel combustion system is lower than in E0 fuel, both in heat transfer processes in the cylinder walls and the engine cooling system. The heat loss of E50 fuel also decreases with increased AFR and engine speed. However, energy losses in the exhaust gas of E50 fuel increase with increasing AFR and engine speed and are higher than E0.
4. The heat in the combustion chamber that is converted to power at the engine output shaft for E50 fuel decreases if the AFR and engine speed increase. It is due to the heat in the cylinder increasing with increasing AFR and PM so that friction losses increase.
5. Some efficiency indicators show that the optimum values of indicative thermal efficiency, brake thermal efficiency, and mechanical efficiency are obtained when using AFR 10:1 for E50 fuel and are better than E0 fuel. However, optimal volumetric efficiency was obtained at AFR 14:1, and the value tends to increase sharply if the engine speed increased.

The result of this research is the application of the principle of the first law of thermodynamics which is focused on the equilibrium of energy quantity. To complement the results of this study, further research will analyze the quality of energy in combustion components through the exergy analysis approach which is an application of the second law of thermodynamics.

## References

1. **Pulkrabek, W. W.** 1997. *Engineering Fundamentals of the Internal Combustion Engine*. New Jersey: Prentice Hall. 411p.
2. **Wang, J.; Huang, F.; Wang, X.; Jiang, X. Z.; Luo, K. H.** 2024. Role of methane in ammonia combustion in air: From microscale to macroscale, *Fuel Processing Technology* 256: 108075. <https://doi.org/10.1016/j.fuproc.2024.108075>.
3. **Rahman, M. M.; Mohammed K. Mohammed, and Rosli A. Bakar.** 2009. Effect of Air Fuel Ratio on Engine Performance of Single Cylinder Port Injection Hydrogen Fueled Engine: A Numerical Study, *Proceedings of the International MultiConference of Engineers and Computer Scientists, II, IMECS Hongkong*.
4. **Zhao, L.; Wang, X.; Wang, D.; Su, X.** 2020. Investigation of the effects of lean mixtures on combustion and particulate emissions in a DISI engine fueled with bioethanol-gasoline blends, *Fuel* 260: 116096. <https://doi.org/10.1016/j.fuel.2019.116096>.
5. **Odunlami, O. A.; Oderinde, O. K.; Akeredolu, F. A.; Sonibare, J. A.; Obanla, O. R.; Ojewumi M. E.** 2022. The effect of air-fuel ratio on tailpipe exhaust emission of motorcycles, *Fuel Communications* 11: 100040. <https://doi.org/10.1016/j.jfueco.2021.100040>.
6. **Almaleki, A.; Hellier, P.; Ladommatos, N.; Talibi, M.; Khan, Z.** 2023. Effects of fuel composition at varying air-fuel ratio on knock resistance during spark-ignition combustion, *Fuel* 344: 128015. <https://doi.org/10.1016/j.fuel.2023.128015>.
7. **Al-Arkawaz, S. A. F.** 2019. Analyzing and predicting the relation between air-fuel ratio (AFR), lambda ( $\lambda$ ), and the exhaust emissions percentages and values of gasoline-fueled vehicles using versatile and portable emissions measurement system tools, *SN Applied Science* 1: 1370. <https://doi.org/10.1007/s42452-019-1392-5>.
8. **Hodonj, D.; Borchers, M.; Zeh, L.; Hoang, G. T.; Tischer, S.; Lott, P.; Deutschmann, O.** 2023. Impact of operation parameters and lambda input signal during lambda-dithering of three-way catalysts for low-temperature performance enhancement, *Applied Catalysis B: Environment and Energy* 345: 123657. <https://doi.org/10.1016/j.apcatb.2023.123657>.
9. **Chan, S. H.** 1996. An Exhaust Emissions Based Air-Fuel Ratio Calculation for Internal Combustion Engines, *Proceedings of the Institution of Mechanical Engineers, Part D: Journal of Automobile Engineering* 210(3): 273-280. [https://doi.org/10.1243/PIME\\_PROC\\_1996\\_210\\_271\\_02](https://doi.org/10.1243/PIME_PROC_1996_210_271_02).
10. **Frasci, E.; Novella Rosa, R.; Pla Moreno, B.; Arsie, I.; Jannelli, E.** 2023. Impact of pre-chamber design and air-fuel ratio on combustion and fuel consumption in a SI engine equipped with a passive TJI, *Fuel* 345: 128265. <https://doi.org/10.1016/j.fuel.2023.128265>.
11. **Vasu, S. S.; Davidson, D. F.; Hanson R. K.** 2008. Jet fuel ignition delay times: Shock tube experiments over wide conditions and surrogate model predictions, *Combustion and Flame* 152(1-2): 125-143. <https://doi.org/10.1016/j.combustflame.2007.06.019>.
12. **Hoang, T.-D. Nghiem, N.** 2021. Recent Developments and Current Status of Commercial Production of Fuel Ethanol, *Fermentation* 7(4): 314. <https://doi.org/10.3390/fermentation7040314>.
13. **Paluri, B; Patel, D.** 2022. Combustion and performance characteristics of SI engine with bioethanol blended fuels, *International Journal of Energy Research* 46(15): 24454-24464. <https://doi.org/10.1002/er.8759>.
14. **Rimkus, A.; Pukalskas, S.; Majeras, G.; Nagurnas, S.** 2024. Impact of Bioethanol Concentration in Gasoline on SI Engine Sustainability, *Sustainability* 16(6): 2397. <https://doi.org/10.3390/su16062397>.
15. **Paloboran, M.; Syam, H.; Yahya, M.; Darmawang.** 2021. The development of combustion strategy in improving the performances of SI-PFI engine using E50 of gasoline-bioethanol fuel blend, *Herald of the Bauman Moscow State Technical University. Series Natural Sciences* 4(97): 115-135. <https://doi.org/10.18698/1812-3368-2021-4-115-135>.
16. **Paloboran, M.; Sutantra, I.N.; Sudarmanta, B.** 2016. Performances and emissions characteristics of three main types composition of gasoline-ethanol blended in

- spark ignition engines, *International Review of Mechanical Engineering (IREME)* 10(7): 552-559.  
<https://doi.org/10.15866/ireme.v10i7.9968>.
17. **Suyatno; Riupassa, H.; Marianingsih, S.; Nanlohy, H., Y.** 2023. Characteristics of SI engine fueled with BE50-Isocetane blends with different ignition timings, *Heliyon* 9(1): e12922.  
<https://doi.org/10.1016/j.heliyon.2023.e12922>.
  18. **Serras-Pereira, J.; Aleiferis, P. G.; Richardson, D.** 2013. An Analysis of the Combustion Behavior of Ethanol, Butanol, Iso-Octane, Gasoline, and Methane in a Direct-Injection Spark-Ignition Research Engine, *Combustion Science and Technology* 185: 484–513.  
<https://doi.org/10.1080/00102202.2012.728650>.
  19. **Frutuoso, F. S.; Alves, C. M. A. C.; Araújo, S. L.; Serra, D. S.; Barros, A. L. B. P.; Cavalcante, F. S. Á.; Araújo, R. S.; Policarpo, N. A.; Oliveira, M. L. M.** 2023. Assessing light flex-fuel vehicle emissions with ethanol/gasoline blends along an urban corridor: A case of Fortaleza/Brazil, *International Journal of Transportation Science and Technology* 12(2): 447-459.  
<https://doi.org/10.1016/j.ijtst.2022.04.001>.
  20. **Pana, C.; Negurescu, N.; Cernat, A.** 2013. Improvement of the Automotive Spark Ignition Engine Performance by Supercharging and Bioethanol Use, *Proceedings of the FISITA 2012 World Automotive Congress* 191: 27-36.  
[https://doi.org/10.1007/978-3-642-33777-2\\_3](https://doi.org/10.1007/978-3-642-33777-2_3).
  21. **Amaral, L. V.; Malaquias, A. C. T.; Fraga, M. A.; Torres, R. B; Sebastiao, R. C. O.; Pujatti, F. J. P.** 2024. Combustion and specific fuel consumption evaluation of a single-cylinder engine fueled with ethanol, gasoline, and a hydrogen-rich mixture, *Case Studies in Thermal Engineering* 57: 104316.  
<https://doi.org/10.1016/j.csite.2024.104316>.
  22. **Flamarz Al-Arkawazi, S. A.; Cameselle, C.** 2019. The gasoline fuel quality impact on fuel consumption, air-fuel ratio (AFR), lambda ( $\lambda$ ) and exhaust emissions of gasoline-fueled vehicles, *Cogent Engineering* 6(1): 1616866.  
<https://doi.org/10.1080/23311916.2019.1616866>.
  23. **Nagy, A. L.; Knaup, J.; Zsoldos, I.** 2018. A Review on the Effect of Alternative Fuels on the Friction and Wear of Internal Combustion Engines, In: Jármai, K., Bolló, B. (eds) *Vehicle and Automotive Engineering* 2: 42–55.  
[https://doi.org/10.1007/978-3-319-75677-6\\_4](https://doi.org/10.1007/978-3-319-75677-6_4).
  24. **Cherwoo, L.; Gupta, I.; Flora, G.; Verma, R.; Kapil, M.; Arya, S. K.; Ravindran, B.; Khoo, K. S.; Bhatia, S. K.; Chang, S. W.; Ngamcharussrivichai, C.; Ashokkumar, V.** 2023. Biofuels an alternative to traditional fossil fuels: A comprehensive review, *Sustainable Energy Technologies and Assessments* 60: 103503.  
<https://doi.org/10.1016/j.seta.2023.103503>.
  25. **Aladayleh, W.; Alahmer, A.** 2015. Recovery of Exhaust Waste Heat for ICE Using the Beta Type Stirling Engine, *Journal of Energy* 2015: 495418.  
<http://dx.doi.org/10.1155/2015/495418>.
  26. **Heywood, J.B.** 1988. *Internal Combustion Engines Fundamentals*, McGraw-Hill, Inc. USA. 930p.
  27. **Szybist, J.; Foster, M.; Moore, W.; Confer, K.; Youngquist, A.; Wagner, R.** 2010. Investigation of Knock Limited Compression Ratio of Ethanol Gasoline Blends, *SAE Technical Paper*: 1-22.  
<https://doi.org/10.4271/2010-01-0619>.
  28. **Al-Breiki, M.; Bicer, Y.** 2023. Liquefied hydrogen vs. liquefied renewable methane: Evaluating energy consumption and infrastructure for sustainable fuels, *Fuel* 350: 128779.  
<https://doi.org/10.1016/j.fuel.2023.128779>.
  29. **Chupka, G. M.; Christensen, E.; Fouts, L.; Alleman, T. L.; Ratcliff, M. A.; McCormick R. L.** 2015. Heat of Vaporization Measurements for Ethanol Blends Up to 50 Volume Percent in Several Hydrocarbon Blendstocks and Implications for Knock in SI Engines, *SAE International Journal of Fuels and Lubricants* 8(2): 251-263.  
<https://doi.org/10.4271/2015-01-0763>.
  30. **Ahmad, M. S.** 2012. Friction and indicated power measurement for diesel engine by aerial dynamometer, *Al-Rafidain Engineering Journal (AREJ)* 20(2): 106-115.  
<https://doi.org/10.33899/rengj.2012.47288>.
  31. **Wang, Y.; Jiang, L.; Liu, H.; Yan, J.; Hočevár M.; Xiang, M.** 2021. Cooling performance and power consumption analysis of automobile engine cooling system, *Energy Sources, Part A: Recovery, Utilization, and Environmental Effects*: 1–17.  
<https://doi.org/10.1080/15567036.2021.1955045>.
  32. **Taha, Y. F.; Khalaf, H. J.; Hamada, K. I.** 2020. An assessment of the availability and efficiency of a gasoline-fueled spark ignition internal combustion engine, *Energy Sources, Part A: Recovery, Utilization, and Environmental Effects*: 1–22.  
<https://doi.org/10.1080/15567036.2020.1825558>.
  33. **Śliwiński, K.; Szramowiat, M.** 2018. Development of cooling systems for internal combustion engines in light of the requirements of modern drive systems, *International Automotive Conference: IOP Conf. Series: Materials Science and Engineering* 421: 1-9.  
<https://doi.org/10.1088/1757-899X/421/4/042078>.
  34. **Adin, M. Ş.; Altun, Ş.; Adin, M. Ş.** 2021. Effect of using bioethanol as fuel on start-up and warm-up exhaust emissions from a diesel power generator, *International Journal of Ambient Energy* 43(1): 5711-5717.  
<https://doi.org/10.1080/01430750.2021.1977387>.
  35. **Menacer, B.; Narayan, S.; Mahroogi, F. O.** 2023. Studying hydrodynamic friction in the oil ring/cylinder liner contact of an internal combustion engine, *Cogent Engineering* 10(2): 2289261.  
<https://doi.org/10.1080/23311916.2023.2289261>.
  36. **Fuc, P.; Merkisz, J.; Lijewski, P.; Merkisz-Guranowska, A.; Ziolkowski, A.** 2014. The assessment of exhaust system energy losses based on the measurements performed under actual traffic conditions, *WIT Transactions on Ecology and the Environment* 190: 369-378.  
<https://doi.org/10.2495/EQ140361>.
  37. **Annamalai, B.; Murugesan, P.; Le, T. T.; Nguyen, P. Q. P.** 2024. Behavior analysis of Low-Heat Rejection engine powered by biodiesel under varied exhaust gas recirculation ratios, *Energy Sources, Part A: Recovery, Utilization, and Environmental Effects* 46(1): 3546-3569.  
<https://doi.org/10.1080/15567036.2024.2319727>.
  38. **Yang, G.; Yin, Z.; Wei, J.; Zeng, Y.; Li, L.; Zhan, R.; Lin, H.** 2023. Physicochemical properties of soot in diesel engine lubricating oil: characterizations and impact on frictional characteristics, *Fullerenes, Nanotubes and Carbon Nanostructures* 32(4): 333–345.  
<https://doi.org/10.1080/1536383X.2023.2282718>.

39. **Taylor, R. I.; Coy, R. C.** 2000. Improved fuel efficiency by lubricant design: a review, *Proceedings of the Institution of Mechanical Engineers, Part J: Journal of Engineering Tribology* 214(1): 1-16.  
<https://doi.org/10.1177/135065010021400101>.
40. **Yang, J.; Du, Y.; Ma, T.** 2024. Assessing the carbon mitigation impact of energy choices in China: a focus on renewable energy and thermal efficiency improvement, *Applied Economics*: 1-18.  
<https://doi.org/10.1080/00036846.2024.2322574>.
41. **Gobbi, M.; Sattar, A.; Palazzetti, R.; Mastinu, G.** 2024. Traction motors for electric vehicles: Maximization of mechanical efficiency – A review, *Applied Energy* 357: 122496.  
<https://doi.org/10.1016/j.apenergy.2023.122496>.
42. **Holman, J. P.** 2012. *Experimental methods for engineers*, 8th edition. New York: McGraw-Hill series in mechanical engineering. 739p.

M. Paloboran, T. A. Pangruruk, Y. Tjandi

#### EVALUATION OF ENERGY CONVERSION AND DISTRIBUTION ON THE SI-PFI ENGINE FUELED BY A GASOLINE-BIOETHANOL BLEND WITH AFR VARIATIONS

#### S u m m a r y

This study aims to investigate the engine performance of spark-ignition engines with port fuel injection using E50 fuel, which contains 50% gasoline and pertalite (in Indonesia) and 50% hydrate bioethanol, at air-fuel ratio variations of 10:1, 12:1, and 14:1. The experiments were conducted using a 1-cylinder, 662 cc engine research test with a constant load of 3 kg and engine speed variations of 1500 and 1800 RPM, as well as a compression ratio of 10:1 and standard ignition timing. The engine ran with E50 fuel, and the experimental results were compared with those of E0 for an air-fuel ratio of 14:1. According to the data, the fuel energy of E50 in an AFR of 14:1 is 0.11 kW higher than that of E0, and it increases by 21.6% when the engine speed increases from 1500 to 1800 RPM. The results also indicate that the efficiency of all performance indicators, such as indicative thermal efficiency, brake thermal efficiency, and mechanical efficiency, is maximized when the engine is operated at an AFR of 10:1 for E50 fuel. Additionally, the volumetric efficiency of E50 reaches its maximum when the fuel is burned at an AFR of 14:1, and it increases as the engine speed increases. However, it should be noted that the brake power decreases due to the frictional power of the fuel increase.

**Keywords:** AFR, energy conversion, gasoline, bio-ethanol, fuel blend, energy.

Received May 4, 2024

Accepted October 22, 2024



This article is an Open Access article distributed under the terms and conditions of the Creative Commons Attribution 4.0 (CC BY 4.0) License (<http://creativecommons.org/licenses/by/4.0/>).